# The Atomistic Modeling of Wave Propagation in Nanocrystals

E.M. Bringa, A. Caro, M. Victoria, and N. Park

*This paper presents non-equilibrium molecular dynamics simulations of wave propagation in nanocrystals. The width of the traveling wave front increases with grain size, d, as $d^{1/2}$. This width also decreases with the pressure behind the front. When the results are extrapolated to micro-crystals, reasonable agreement with experimental data is obtained. In addition, this extrapolation agrees with models that only take into account the various velocities of propagation along different crystalline orientations without including grain boundary effects. The results indicate that, even at the nanoscale, the role of grain boundaries as scattering centers or as sources of plasticity does not increase significantly the width of the traveling wave.*

## INTRODUCTION

Nanocrystals have been extensively studied, both in experiments[1] and simulations,[2–4] for their numerous beneficial properties such as strength. In general, continuum-scale plasticity models only include polycrystalline effects by averaging over various crystalline directions to obtain some effective isotropic material.[5] There are several models that do include full polycrystalline anisotropy, but where grain boundaries (GB) are considered infinitesimally thin or not influencing the deformation of the material.[6] Few recent models have tried to incorporate the role of grain boundaries,[7,8] but the connection to atomic-scale processes has only recently begun to emerge.[9]

Many current experiments[1] and most atomistic simulations on nanocrystals[2–4] involve homogeneous deformation of the material (i.e., the whole system is subjected to the same deformation). However, there may be instances, especially at very high strain rates, where this would be no longer true;[10] a wave will travel through the material with deformed material behind the wave front. This article will focus on how the nanocrystalline structure can change the wave propagation due to polycrystalline effects. It is important to understand in detail the response of polycrystalline materials to wave propagation for a number of applications. For instance, the National Ignition Facility (NIF)[11] at Lawrence Livermore National Laboratory will require polycrystalline ignition targets where the wave front has to be extremely smooth to avoid Rayleigh-Taylor[12] instabilities caused by perturbations due to the grain structure. Such instabilities can grow, resulting in a final compression diminished below the desired value.

**A polycrystal introduces different wave velocities in each grain, with preferred wave propagation directions.**

Numerous studies, both experimental[13–16] and continuum modeling,[10,17–23] have been conducted on wave propagation in polycrystals, and samples with different grain size do show grain-size dependence in wave propagation.[13,16,18,21] However, models that include atomic-level information are lacking. Figure 1 shows a schematic of a wave traversing a polycrystal. In Figure 1a, the wave is crossing a single crystal and the wave front is "straight" since there are no perturbations (except for possible plasticity or phase transformations). A polycrystal introduces different wave velocities in each grain, with preferred wave propagation directions, as shown in Figure 1b. This fact alone would greatly enhance the wave front width if the difference between propagation velocities is not negligible. For instance, for many face-centered cubic (fcc) metals, the sound velocity along the fast direction can be 10–25% greater than the velocity along the slow direction.[17,18,24] Some models do include the role of anisotropy leading to refraction of the wave, for instance, by increasing the effective path it travels.[18]

In addition to the polycrystal anisotropy, GB could play a role as scattering centers, or barriers to the wave transmission, with a fraction of the wave dissipated as indicated in Figure 1c. Figure 1d shows that GB can also be sources of dislocations where the plastic deformation may change the width of the wave front. Several calculations[17,18,21] estimate the effect sketched in Figure 1b, but no analytical or semi-analytical models predict shock width for a given grain size. Although there have been a few studies for single grain boundaries,[25,26] there are no studies regarding the effects sketched in Figure 1c and d in polycrystals. Based on Figure 1, the general expression of the width of the front, $\Delta z$, could be assumed to be the sum of (as a first approximation) independent contributions from Figure 1b–c:

$$\Delta z = \Delta z_{aniso} + \Delta z_{GBscatt} + \Delta z_{plastic} \qquad (1)$$

An upper estimate of $\Delta z_{aniso}$ can be obtained from a two-dimensional (2-D) propagation case as follows. Imagine two rows of grains, one consisting only of grains where the velocity is slow and the other where the velocity is fast. The

spread Δz of the front after a time t will be Δv t, where Δv is the velocity differential. For a sample of fixed length L, with grains of size d, $L/d = N_g$ is the mean number of traversed grains, and $t = L/\langle v \rangle$. Therefore,

$$\Delta z = (\Delta v/\langle v \rangle)\, d\, N_g = A_v\, d\, N_g \qquad (2)$$

where $(\Delta v/\langle v \rangle) = A_v$ is called the anisotropy factor. For a sample with many rows and grains of size d, with the same number of slow and fast grains randomly distributed, one would still expect a linear dependence of Δz with the anisotropy factor. However, there will be a large number of rows where the number of slow and fast grains will be roughly the same, giving $\Delta z_{aniso} \sim 0$. Assuming a power law form for the grain size dependence, $d^{\alpha}$, this would give a dependence with $\alpha < 1$. The fact that the shock width increases with grain size has been experimentally observed for metals[13] and oxides.[16] Recent modeling[21] of this process for wave propagation in beryllium polycrystals gave $\alpha \sim 1/2$. Note that Equation 2 also predicts that a wave will continue widening with time or as it traverses more and more grains.

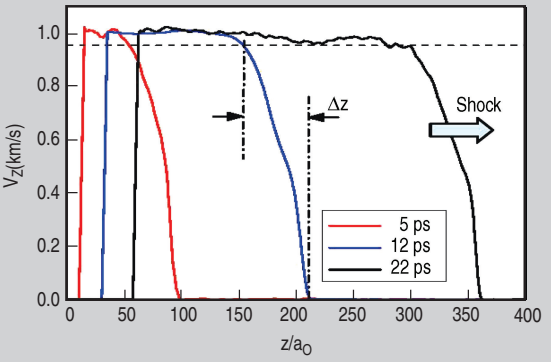


Figure 3. Three snapshots from an MD simulation for d = 20 nm and P = 47 GPa showing velocity profiles, averaged in slices one lattice parameter, $a_0$, thick, perpendicular to the shock propagation direction. The measurement of the width Δz at t = 12 ps is indicated.

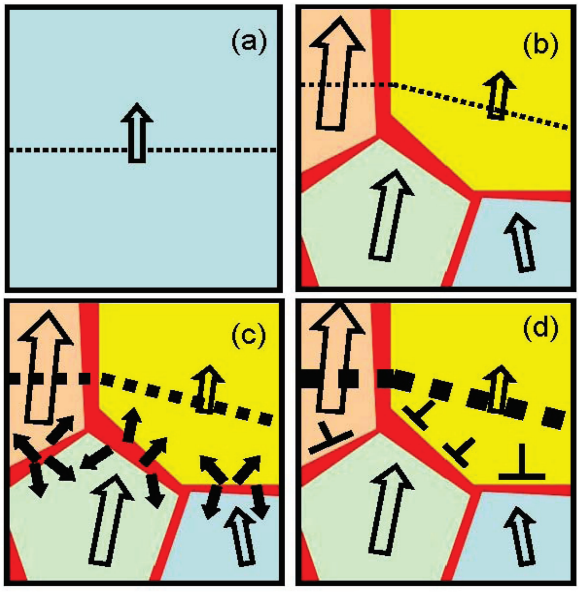


Figure 1. A schematic of wave propagation in a polycrystal. The dotted line indicates the wave front. (a) single crystal, (b–d) polycrystals showing: (b) anisotropy due to different crystalline orientations, (c) GB acting as scattering centers, and (d) GB enhancing plasticity induced by the wave front.

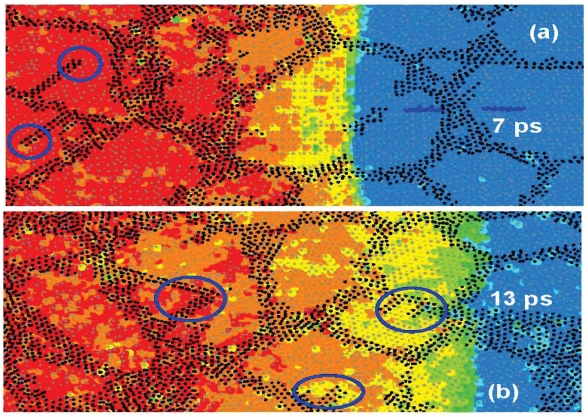


Figure 2. Snapshots of the MD simulation that show the wave front at two different times and at two different locations in the same sample. Grain boundary atoms are overlapped as small black dots. d = 5 nm, P = 22 GPa, $U_p$ = 0.5 km/s and 10% strain. Atoms are colored according to their kinetic energy (red, high-moving at $U_p$; blue, low-unshocked). The upper frame shows a sharp front inside the grains, with some refraction due to orientation. The energy levels track the GB, and in frame (b) the front itself tracks the shape of one of the grains. Some of the stacking faults generated by the wave are marked with blue circles.

## ATOMISTIC SIMULATIONS

Typical GBs in real materials are only ~1 nm thick and are difficult to model using continuum models. In this study, the authors use the massively parallel code MDCASK[27] to carry out atomistic molecular dynamics (MD) simulations of embedded-atom method (EAM) copper samples.[28] Prismatic samples were built using the Voronoi construction with random texture.[3] Dislocation cores were identified using a centro-symmetry parameter filter.[29] The study focused on the propagation of waves moving faster than the speed of sound (i.e., shock waves). There are numerous MD simulations of shocks in single crystals,[24,30–32] but only a limited number on polycrystalline materials.[31–33] The authors have simulated samples with 0.5–64 million atoms, and average grain sizes of 5 nm, 10 nm, and 20 nm on 32–768 central processing units. Further analysis of these simulation results is in progress and will be published elsewhere.[33]

The samples had free surfaces along the shock wave direction and periodic boundary conditions in the transverse direction. The first few surface layers on one side were chosen as a piston. A step velocity function was applied to these piston atoms at the desired piston velocity, $U_p$, to create a traveling wave with velocity $U_s$.[24] The stress along the shock direction (the shock pressure) behind the front is given by the Hugoniot equations[30]

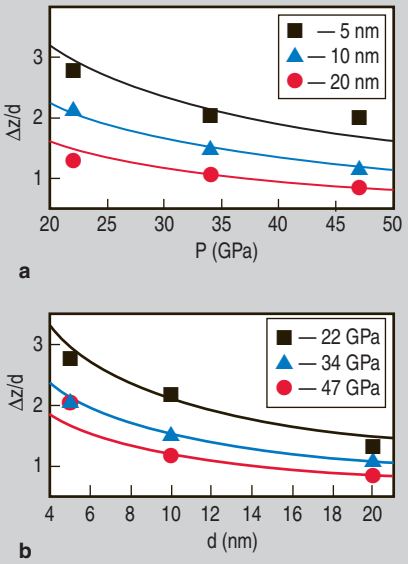


Figure 4. Front width, normalized to the grain size, versus (a) pressure and (b) grain size. Solid lines show the fitting from Equation 3. Width was measured when the wave front had traveled ~70 nm.

dealing with mass, momentum, and energy conservation at the front: $P_H = \rho_0 U_p U_s$. The strain behind the front is constant and given by $\varepsilon = U_p/U_s$. Assuming a linear Hugoniot relationship, $U_s = c_0 + s_1 U_p$. For copper, $c_0 = 4.0$ km/s and $s_1 = 1.5$.[24] The MD simulations[24] found that this equation is a reasonable approximation for this EAM potential, especially for strong shocks.

Figure 2 shows snapshots of a simulation with d ~ 5 nm and P = 22 GPa (strain is ~10%). Despite the small grain size, significant dislocation activity is observed, driven by the large applied stress. Partial dislocations are emitted from the GB and cross the grain leaving a stacking fault behind,[33] as in the previous homogeneous deformation simulations of larger grains.[2,3] Given the large level of plastic activity, one could expect strong influences at the shock front for the simulated cases, as suggested in Figure 1d. In addition, both frames of Figure 2 show refraction of the wave, as seen in Figure 1b.

Figure 3 shows several snapshots of the velocity profiles in one of the simulations. As the piston advances, the wave front advances, too, at a faster velocity. The piston drive is a step function, but the wave front develops a characteristic width, which is related to the gradient in kinetic energy (velocity) observed in Figure 2. A working definition of width is the distance between the edge of the front and the point where the velocity is 95% $U_p$, as shown in Figure 3. The profile in Figure 3 has been averaged perpendicularly to the propagation direction over about ten grains. However, the width of the wave can be identified along the shock direction with the width of the fluctuations normal to the direction of propagation. Close inspection of simulation snapshots, like those in Figure 2, shows that this identification is roughly valid.

Figure 4 shows the width, normalized to the grain size, versus pressure and grain size. A simple functional form has been adapted to fit the calculations in this work. For copper, $A_v \sim 0.25$ will depend on pressure only weakly in the interval studied and it is assumed constant. Assuming a power law behavior with grain size and pressure, the observed width can be fit using the following relationship:

$$\Delta z/d = C\, A_v\, (d/d_o)^{\alpha}\, (P/P_o)^{\beta} \qquad (3)$$

Setting $d_o = 10$ nm and $P_o = 47$ GPa, the data is fit to get $C \sim 5.4$, $\alpha \sim -1/2$, and $\beta \sim -3/4$. As the shock pressure increases, plasticity also increases, but the overall result is a decrease in the width of the front, as seen in experiments and predicted by viscoplastic models.[34] This leads to a steep increase of the strain rate with pressure, as measured for strong, overdriven shocks. As mentioned previously, the $d^{1/2}$ grain size dependence is the same dependence that was recently found in simulations[21] of micro-scale polycrystalline beryllium which did not include GB effects, indicating that this dependence may be somewhat general and that the role of GBs may be relatively small for all cases. In fact, dislocation activity does not seem to significantly widen the relatively sharp front inside grains, as seen in Figure 2.

A continuum-level model has shown that the wave front width actually increases with time[17] (i.e., the irregularities in the front are enhanced as the wave traverses more grains). Experimental data, however, remains scarce and gives only marginal effects.[14,15] Figure 5 shows results for samples that are ~400 fcc cells (~150 nm) long. After a transient stage, a steady-state increase in width is reached, which can be modeled with a power law fit including the number of grains, as:

$$\Delta z/d = C\, A_v\, (d/d_o)^{-1/2}\, (P/P_o)^{-3/4}\, (N_g/N_{go})^{\gamma} \qquad (4)$$

with $N_{go} \sim 1$ for the 20 nm grains, with $\gamma \sim 1/5$. The length of the samples may be too small to carry out an appropriate fitting of this dependence. A fit to the continuum model results in Reference 15 gives $\gamma \sim 1/2$.

## WAVE PROPAGATION IN MICROMETER-SIZED GRAINS

From Figures 4 and 5, a simple analytical form can be obtained that agrees with the simulation data. However, given the relatively small simulation data set and the narrow range of grain sizes and pressures accessible to atomistic simulations, it may not be valid to extrapolate these results to the micro-scale. Chhabildas and Asay[14] measured an upper limit to the rise time of shocks in copper targets with d ~ 5 μm at a few different

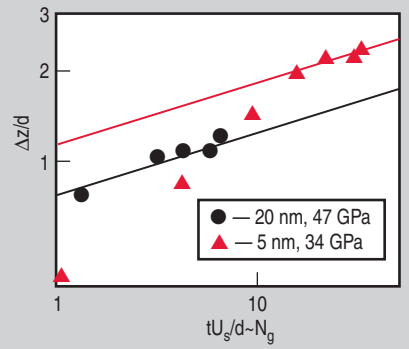


Figure 5. Evolution of the width with scaled time for two simulated cases showing the power law evolution that gives $\gamma = 1/5$.

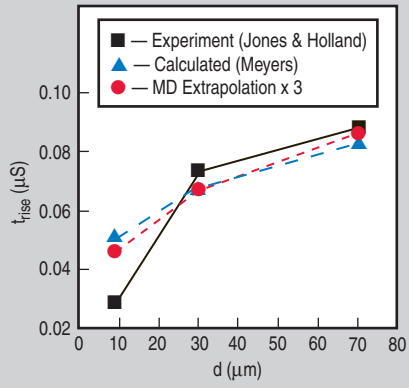


Figure 6. Experimental results[13] compared to the continuum level model by Meyers[18] and the extrapolation of MD results using Equation 4.

pressures. They obtained times of 1.4–2.2 ns, close to their experimental resolution, while the model in this study gives times that are 15–25 times smaller. A worst-case scenario for the model would occur for grain sizes larger than 1 μm at low shock pressure, where the width is expected to be large. Figure 6 shows experimental data for the elastic wave in such a case. Calculations from a numerical model by Meyers,[18] which only includes anisotropies as in Figure 1b, without GB effects, are also shown. Extrapolation of the simulation data to the experimental conditions for a nickel disk of ~19 mm[13] is shown in Figure 6, using $A_v \sim 0.17$ for nickel in Equation 4 and $t_{rise} = \Delta z/U_s$. Results are obtained that are lower by a factor of ~3 than the experimental results and the continuum-level model.

That these results are of the same order could be considered fortuitous, given the simple functional form used, the extrapolation from nano- to micro-scale, and the change of material from copper to nickel. However, the fact that the continuum model has the same behavior with grain size likely indicates that the same basic governing principles are at play here. Since that model only considers the first term in Equation 1 (i.e., the anisotropy in the velocity of propagation of the wave for different grains), this term appears to dominate the development of the width of the wave front. In the simulations, this seems to be the case even for nanostructured materials where one would expect the other two terms in Equation 1 to contribute relatively more than in micrometer-sized materials. On the other hand, copper has a particularly high anisotropy factor, which could mask the role of the GB-related terms in developing the width of the front.

The results may be relevant to the design of NIF targets using micrometer-sized grains. Since anisotropy dominates the extent of the shock width, using targets with preferential texture, such as the candidate beryllium targets[21] ($A_v \sim 0.1$), would significantly reduce fluctuations at the shock front. The same effect would be achieved using a target with a polycrystalline material having small sound velocity anisotropies, as in the case of polycrystalline carbon ($A_v \sim 0$).[35] Future simulations of wave propagation in nanocrystals with hexagonal close packed and diamond crystalline structures, and with different values of the anisotropy parameter, are needed to assess the range of applicability of these findings which use fcc copper nanocrystals. Furthermore, a new generation of interferometry techniques[15,36,37] will allow for improved measurements of shock width, including the possible role of fluctuations.[36]

## CONCLUSION

The width of the wave is a function of grain size, pressure, and time. Simple analytical fits show the same scaling with grain size as models not including GB effects[21] (i.e., as $d^{1/2}$). In addition, extrapolation to micro-scale experiments[13] and models[18] shows reasonable agreement. The simulations suggest that the effect of GB on the width of the wave front is small compared to the effect of anisotropy from crystal to crystal. As a result, continuum-level models of wave propagation could provide front widths not significantly different from those in more computationally expensive atomistic simulations. Additional MD simulations in nanomaterials are needed to establish the soundness of this hypothesis, including materials with low anisotropy. These simulations would allow more accurate power-law fits and possibly a better understanding of the origin of the exponents governing shock width. Finally, despite the limitations of atomistic simulations, the results clearly show that nanocrystalline NIF targets would guarantee small fluctuations in the shock front, decreasing the probability of unwelcome instabilities.[12]

## ACKNOWLEDGEMENT

*The authors would like to thank A. Hamza and R. Cook for fruitful discussions. The work at Lawrence Livermore National Laboratory was performed under the auspices of the U.S. Department of Energy and Lawrence Livermore National Laboratory under contract No. W-7405-Eng-48, LDRD 04-ERD-021.*

## References

1. J.R. Weertman, *Nanostructured Materials: Processing Properties and Potential Applications*, ed. C.C. Koch (Norwich, NY: William Andrew, 2001), pp. 397–421.
2. J. Schiøtz and K.W. Jacobsen, *Science,* 301 (2003), p. 1357.
3. H. Van Swygenhoven et al., *Phys. Rev. B,* 60 (1999), p. 22.
4. V. Yamakov et al., *Nature Materials,* 1 (2002), p. 1.
5. M.A. Meyers and K.K. Chawla, *Mechanical Behavior of Materials* (New York: Prentice Hall, 1998).
6. R.A. Lebensohn and C.N. Tomé, *Acta Metall. Mater.,* 41 (1993), p. 2611.
7. H.H. Fu, D.J. Benson, and M.A. Meyers, *Acta Mater.,* 52 (2004), p. 4413.
8. B. Jiang and G.J. Weng, *J. Mech. Phys. Solids,* 52 (2004), p. 25.
9. A.C. Lund and C.A. Schuh, *Acta Mater.,* 53 (2005), p. 3193.
10. B. Remington et. al., *Met. Mat. Trans. A,* 35 (2004), p. 2587.
11. T.R. Dittrich et al., *Laser and Particle Beams,* 17 (1999), p. 217.
12. J.D. Colvin et al., *J. Appl. Phys.,* 93 (2003), p. 5287.
13. O.E. Jones and J.R. Holland, *Acta Metall.,* 16 (1968), p. 1037.
14. L. Chhabildas and J. Asay, *J. Appl. Phys.,* 50 (1979), p. 2749.
15. K.T. Gagahan et al., *Phys. Rev. Lett.,* 85 (2000), p. 3205.
16. N.K. Bourne et al., *Proc. Royal Soc. London A,* 446 (1994), p. 309.
17. M.A. Meyers and M.S. Carvalho, *Mat. Sci. Eng.,* 24 (1976), p. 131.
18. M.A. Meyers, *Mat. Sci. Eng.,* 30 (1977), p. 99.
19. D.J. Benson, *Wave Motion,* 21 (1995), p. 85.
20. K. Yano and Y. Horie, *Phys. Rev. B,* 59 (1999), p. 13672.
21. R.C. Cook, *Fusion Sci. Technol.,* 41 (2002), p. 155.
22. J.D. Clayton, *J. Mech. Phys. Sol.,* 53 (2004), p. 261.
23. Z. Zhao, R. Radovitzky, and A. Cuitino, *Acta Mater.,* 52 (2004), p. 5791.
24. E.M. Bringa et al., *J. Appl. Phys.,* 96 (2004), p. 3793.
25. D.S. Ivanov et al., *Shock Compression of Condensed Matter-2003,* ed. M.D. Furnish, Y.M. Gupta, and J.W. Forbes (New York: APS, 2004), pp. 225–228.
26. P.K. Schelling, S.R. Phillpot, and P. Keblinski, *J. Appl. Phys.,* 95 (2004), p. 6082.
27. MDCASK: *http://www.llnl.gov/asci/purple/benchmarks/limited/mdcask/*
28. Y. Mishin et al., *Phys. Rev. B,* 63 (2001), p. 224106.
29. C.L. Kelchner, S.J. Plimpton, and J.C. Hamilton, *Phys. Rev. B,* 58 (1998), p. 11085.
30. L. Holian and P.S. Lomdahl, *Science,* 280 (1998), p. 2085.
31. K. Kadau et al., *Science,* 296 (2002), p. 1681.
32. F.A. Sapozhnikov, V.V. Dremov, and M.S. Smirnova, *J. Phys. IV France,* 110 (2003), p. 323.
33. E.M. Bringa et al., submitted to *Science* (2005).
34. A. Molinari and G. Ravichandran, *J. Appl. Phys.,* 95 (2004), p. 1718.
35. J.K. Krüger et al., *Diamond and Related Mat.,* 9 (2000), p. 123.
36. Yu.I. Mescheryakov, N.A. Mahutov, and S.A. Atroshenko, *J. Mech. Phys. Solids,* 42 (1994), p. 1435.
37. M. Hauer et al., *Thin Solid Films,* 453 (2004), p. 584.

*E.M. Bringa, A. Caro, and M. Victoria are with Lawrence Livermore National Laboratory in Livermore, California. N. Park is with Atomic Weapons Establishment in Berkshire, United Kingdom.*

**For more information, contact E.M. Bringa, Lawrence Livermore National Laboratory, 7000 East Avenue, Livermore CA 94550, USA; (925) 423-5724; fax (925) 422-4665; e-mail ebringa@llnl.gov.**